



AB Initio Study of Coinage Metal Doped Graphene Nano Ribbons

Research Article

Pankaj Srivastava¹, Subhra Dhar^{1,*} and Neeraj K. Jaiswal²

¹ Nanomaterials Research Group, ABV-Indian Institute of Information Technology and Management (IIITM), Gwalior 474015, India

² Discipline of Physics, PDPM-Indian Institute of Information Technology, Design and Manufacturing (IIITDM), Jabalpur 482005, India

*Corresponding author: sdharmos@gmail.com

Abstract. The electronic and transport properties of both *zigzag graphene nanoribbons* (ZGNRs) and *armchair graphene nanoribbons* (AGNRs) doped with coinage metals (CM) Cu, Au and Ag has been investigated by employing *ab-initio* approach using non equilibrium Green's function combined with density functional theory. In Cu-doped ZGNRs, it is observed that the linear positive bias I–V curve and conductance is higher due to doping towards the centre of the ribbon. Doping at strategic positions yield currents such that the semiconductor to metal transition takes place in all the Cu-doped AGNRs. Au-doped ZGNRs exhibit stable structure and semimetallic nature is predicted with a high DOS peak distributed over a narrow energy region at the Fermi level. Our calculations for the magnetic properties predict that Au functionalization leads to semiconducting nature with different band gaps for spin up and spin down. Au-doped AGNRs are semiconducting with lower total energy for the FM configuration, and the I-V characteristics reveal semiconductor to metal transition. The spin injection is voltage controlled in all the investigated Au-doped AGNRs. The transmission spectrum (T.S) of Ag-doped ZGNRs present heightened electronic activity due to interaction between Ag impurities and edge states of the ZGNRs. Significant transport properties applicable for various device applications at the nano-regime are thus reported in all the coinage metal doped GNRs.

Keywords. Graphene; Zigzag; Armchair; Copper; Gold; Silver; Electronic; Transport; Spin

PACS. 72.25; 72.80

Received: February 12, 2015

Accepted: November 28, 2015

1. Introduction

Graphene nanoribbons (GNRs) have attracted immense attention in recent years due to their outstanding structural and electronic properties enhancing their appeal for potential applications in nanoelectronic devices. As the characteristics of GNRs depend strongly on their size and shape of their edges, one can obtain metals or semiconductors with an energy gap depending on the ribbon width by controlling the size and edge shape. The study of quantum transport in GNRs is of particular interest for the development of novel nanoelectronic devices since the transport characteristics of nanostructured graphene based devices are affected by the geometry of the GNR edges. The chemical doping of graphene and GNRs is considered as an efficient route able to alter the electronic and quantum transport properties of graphene-like materials [1]. In addition to the chemical nature of the dopant, the location of the doping atoms in the structure and the dopant concentration are very important factors that control the properties of doped GNRs [1]. Approaches that considerably influence the features of GNRs include edge modifications, substitution and adsorption are theoretically and experimentally proposed to functionalize GNRs [2]. For single impurity doping, though substitutional doping is energetically more stable [3] it is established that adsorption is more promising than substitution because of its unrestricted adsorption site and flexible mechanics, thus being easier to control in experiment [2]. As not much study has been done in case of coinage metals (CM)-doped GNR, the authors in this work engage in Cu, Au and Ag, for substitutional doping as well as adsorption in the GNRs. In this work, we study the electronic and transport properties of CM doped GNRs in different configurations by employing *density functional theory* (DFT) based first-principles calculations. We also probe the effects of spin polarization on the electronic and transport properties adsorbed/substituted GNRs and compare the findings with spin compensated calculations. CM substitution and adsorption is modeled on the edge-passivated GNRs. Section 2 discusses the methodology used to obtain the presented results of the structures. The results and discussion is presented in Section 3 and the conclusions are summarized in Section 4.

2. Computational Method

Density functional theory (DFT) based first principles calculations are employed to explore various properties of CM doped GNRs. *Atomistix Tool Kit Virtual NanoLab* (ATK-VNL) simulation package [4] is used for the calculations. We refer to a GNR with N_A dimer lines as a N_A -AGNR and a GNR with N_Z zigzag chains as a N_Z -ZGNR. The schematic diagram of the GNRs and the convention of ribbon width have been shown in Figures 1 and 2. To model the ribbons, supercell method is used and the cutoff energy of 150 Ry is selected to achieve precise results. The investigated ribbons are optimized self-consistently, and all the atoms are fully relaxed so that the maximum force component on all atoms is less than 0.05 eV/Å. The ribbons are allowed to grow along z-axis, whereas the rest of the two directions are confined. We consider the two-probe geometry system within the framework of nonequilibrium Green's function technique where the system is divided into three parts, namely, left and right electrode as well as a central scattering region. In order to obtain I-V characteristics for the two systems, self-consistent calculations were performed in a bias voltage range from 0V to 2.0 V. At each bias voltage, the electronic structure is self-consistently obtained under nonequilibrium conditions.

The transmission spectrum is calculated from,

$$T = T_r(\Gamma_R G_C^R \Gamma_L G_C^A), \tag{2.1}$$

where G_C^R and G_C^A are the retarded and advanced Green's functions of the conductor, respectively and $\Gamma_{R(L)}$ is the coupling matrices from the scattering region to the right (left) lead. Within the NEGF formalism, the $\Gamma_{L(R)}$ becomes

$$\Gamma_L = i[E_L - E_{L+}] \quad \text{and} \quad \Gamma_R = i[E_R - E_{R+}], \tag{2.2}$$

where E_L and E_R are the self energies describing the coupling of the left and right electrode to the semi infinite electrodes [5].

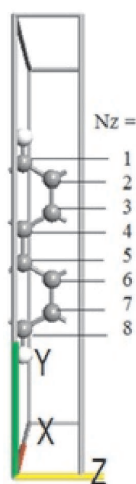


Figure 1. The schematic representation of super cell and the convention of defining the ribbon width for pristine ZGNR (NZ=8).

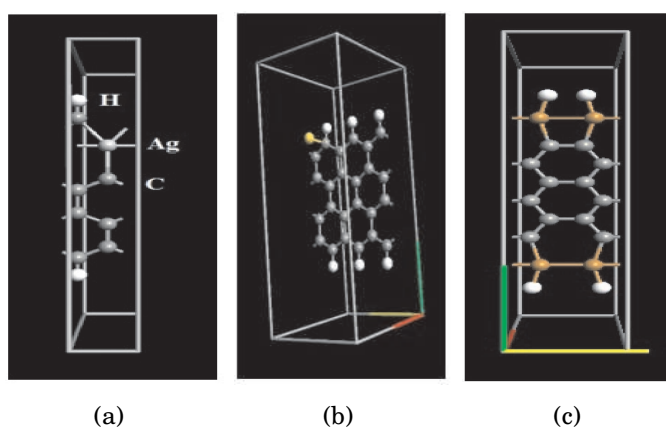


Figure 2. The optimized geometry of the investigated GNRs due to (a) Ag at position 2 (b) Au adsorbed in bridge site (c) Cu at both edges.

3. Result and Discussion

3.1 Cu-doped GNRs

We evaluate the transport properties of the Cu-doped ZGNRs and AGNRs, and perform self consistent calculations to obtain the current-voltage (I-V) characteristics for the bias voltage = 0 V to 2 V for various doping sites. The findings are compared with pristine ribbons and are shown in Figures 3 and 4. Transport properties of ZGNR under low bias are determined by the π/π^* state related to the edge states [6]. At zero bias, the device shows zero current for all the cases, but on increasing the applied bias, prominent changes with regard to the doping sites in all the GNRs is observed. Due to a band gap induced by edge Cu-doping at the centre of the ribbon, in Figure 3(a,b) we observe decrease in the current at low bias [7]. The presence of Cu dopant closer to the centre of the ribbon as well as at the centre of the ribbon raises the metallicity of the ZGNR. In the centre doped ribbon, we find that the current increases with applied bias, but on doping layers closer to the centre (position 3), we observe a linear increase and maximum current obtained, whereas in case of position 2 Cu-doping, NDR after 1V is observed. For all doped AGNRs, in (Figure 3(b) we find that at low bias [6] the current increases

rapidly as bias increases. At further increase of applied bias, we observe the current attains a peak value and decreases thereafter. In both edge Cu-doped AGNR, at biases higher than 1V, the current becomes constant at $350 \text{ \AA}\mu\text{A}$ and NDR behavior starts beyond 2 V. The differential conductances at bias V for 8-ZGNRs and 8-AGNRs doped with Cu atom at top edge, position 2, position 3, centre, both edges, and pristine have been depicted in Figure 4(a,b) respectively. In Figure 4(a) the zigzag ribbon shows *negative differential conductance* (NDC) with position 2 Cu-doped ribbons. At very low biases, edge doping at top edge and both edges have similar effect whereas at higher biases notable result is not observed. Doping AGNRs with Cu at the top edge, position 2, position 3, centre, both edges, and pristine in Figure 3(b) nontrivially influences the conduction mechanism of ribbons as the existence of a NDC is observed in all the Cu-doped AGNRs due to the lowering of currents at higher bias as confirmed by the I-V characteristics. Thus, Cu-doped ZGNRs offer moderate conductances whereas Cu-doped AGNRs offer enhanced conductance along with negative differential conductance over the range of applied bias taken up in this study. As the I-V characteristics of the Cu-doped GNRs include regions of linearity, negative differential regions, saturations, positional Cu-doping may be exploited for various applications.

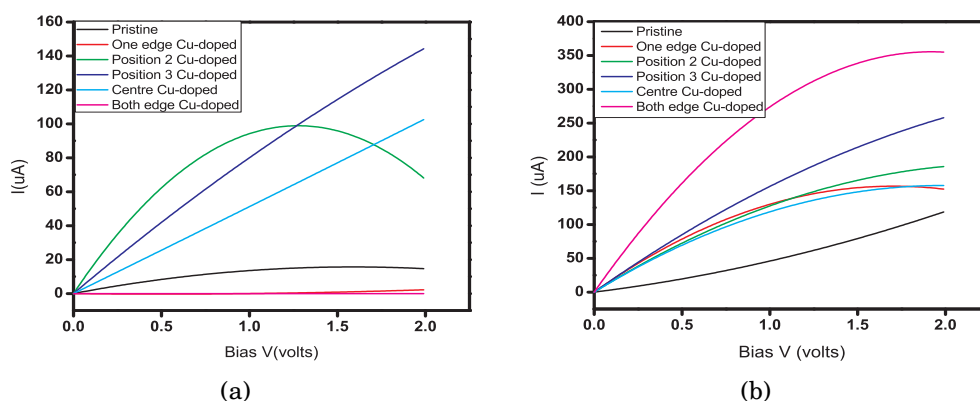


Figure 3. The I-V characteristics of (a) 8-ZGNR and (b) 8-AGNR doped with Cu at top edge, position 2, position 3, centre, and both edges are shown.

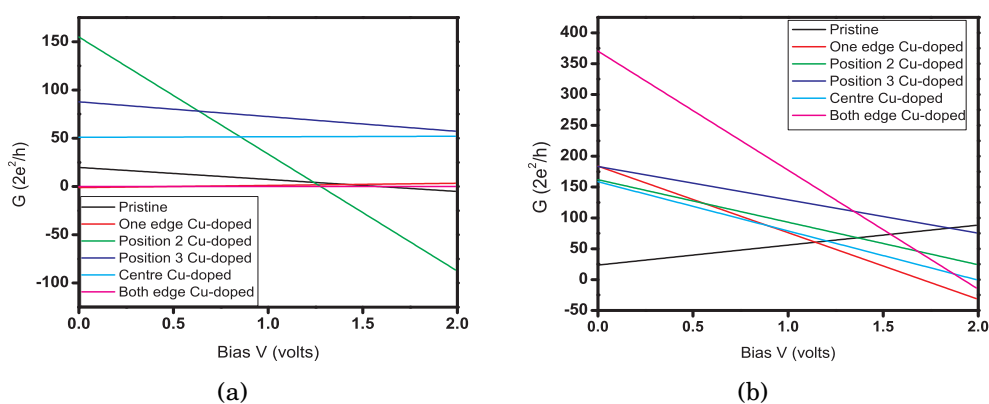


Figure 4. The differential conductance at bias V for (a) 8-ZGNRs and (b) 8-AGNRs doped with Cu at top edge, position 2, position 3, centre and both edges are shown.

3.2 Au-doped GNRs

Since electronic transport properties and the interactions in the Au-graphene systems are not fully understood so far, the authors seek to probe the interactions between Au doping properties and GNRs further in this work. Upon adsorption, in case of top site Au-doped ZGNR, we find that a large negative B.E of -2.41 eV indicates stable and stronger binding of Au with ZGNR (Table 1). The minimum energy configuration for a single gold atom is found to be directly above a carbon atom which is consistent with previous reports in [8]. Binding energy calculations of optimized structures confirm that the edge site is the most preferred site for Au doping in ZGNRs [9]. Figure 5 presents the transmission spectra of Au-adsorbed ZGNR and DOS characteristics which are found to be in confirmation to each other. In particular, transport turns out to be significantly suppressed at energies around the Fermi level at 0 V, with a resulting transport gap. With Au-adsorbed at the top site, we find increased electron transport at Fermi level (as also seen in band structures), but beyond the Fermi level at lower energies we observe zero transport as evident in the DOS characteristics. On increasing the bias, the transmittance maintains more or less a steady value of 2. As most transport of electron occurs around the Fermi level, in case of Au-adsorption, we come across a very high value of DOS at the Fermi level, indicating more states available for occupation. A high DOS peak distributed over a narrow energy region at the Fermi level, confirms semi metallic nature of the Au-adsorbed ZGNR. The spin-oriented band gaps of Au-substituted and Au-adsorbed ZGNR in eV are presented in the Table 1. In all the adsorbed Au FM configurations, we find the bandgaps of the spin up have broadened, whereas the band gaps of the spin down have reduced. This may be attributed to the symmetric Au adsorption at the edge. These results indicate that the doping of Au atoms into different sites considerably alters the electronic structure of ZGNRs. Further, we have performed spin polarized calculations on the substituted and adsorbed Au-doped AGNRs to get an insight into the favored positions of the Au atom in all the investigated configurations. In case of Au-adsorption at atop site, we find that the FM states are more stable as compared to corresponding AFM states, indicating that the FM configurations are the ground states in confirmation to earlier findings in [10]. On calculating the efficiency of the two probe device characterized by the injection of the spin current, we find that both the FM and AFM configurations exhibit 70% and 78% spin polarized respectively at 1V. Figure 6 shows the degree of spin injection as a function of applied bias (V) of the Au-adsorbed AGNR. We also find that on lowering the applied bias to 0.5 V, a large spin polarization of 95% could be achieved in these systems. Therefore, the spin injection is voltage controlled in all the investigated Au-doped AGNRs.

Table 1. Spin polarised band gaps and B.Es of Au adsorbed ZGNRs.

Au doped 8-ZGNR Configuration	Band gap FM (eV)		Band gap AFM (eV)		Binding Energy (eV)	
	spin up	spin down	spin up	spin down		
Adsorbed atop	1.0	1.03	1.02	0.94	-2.41	-0.79 [11]
Adsorbed bridge	0.91	1.03	1.19	1.14	-2.40	-0.74 [11]
Adsorbed hole site	0.96	1.02	1.02	0.96	-2.40	-0.52 [11]

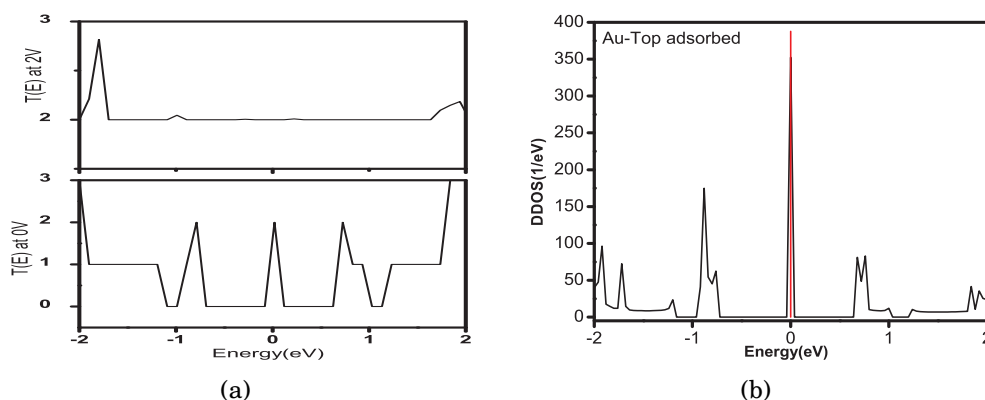


Figure 5. The (a) transmission spectra and (b) device density of states for 8-ZGNR with Au adsorbed at top site.

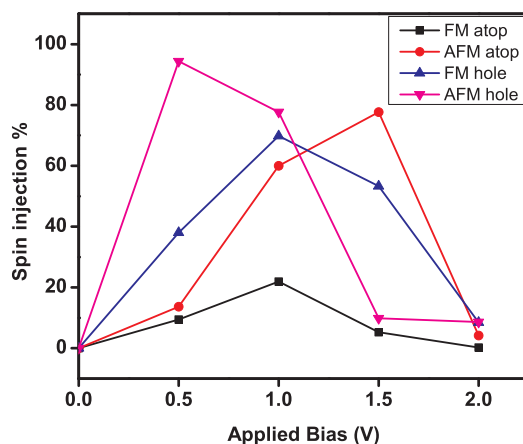


Figure 6. The degree of spin injection as a function of applied bias (V) of the Au-adsorbed AGNR.

3.3 Ag-doped GNRs

To explore the transport properties of Ag-doped two-probe system, specific to ZGNR with $N = 8$, the *transmission spectrums* (T.S) of the Ag doped ZGNRs are calculated at zero bias, compared with pristine ribbons and presented in Figure 7. Across the Fermi level, on tuning the site of Ag doping, heightened electronic activity is observed on doping the ZGNR with Ag at the identified sites. This behavior may be attributed to the interaction between Ag impurities and edge states of ZGNRs, which governs the electron occupation of the edge states. We calculated the I-V characteristics at zero bias, at finite biases of 1 V and 2 V of the Ag-doped ribbons and is presented in Figure 8. On varying the current as a function of applied voltage for position dependent impurities of Ag in 8ZGNR, it is observed that the current increases non linearly and attains a current of $60 \text{ \AA}\mu\text{A}$ at 2 V for site 2 doping which is closer to the edge of the ribbon. The *negative differential resistance* (NDR) effect is also observed in this case. In case of site 3 Ag-doped ZGNR, the highest current attained is $130 \text{ \AA}\mu\text{A}$ at 2 V, which is encouraging enough to conclude that the Ag doped ZGNR can be used as versatile electronic device.

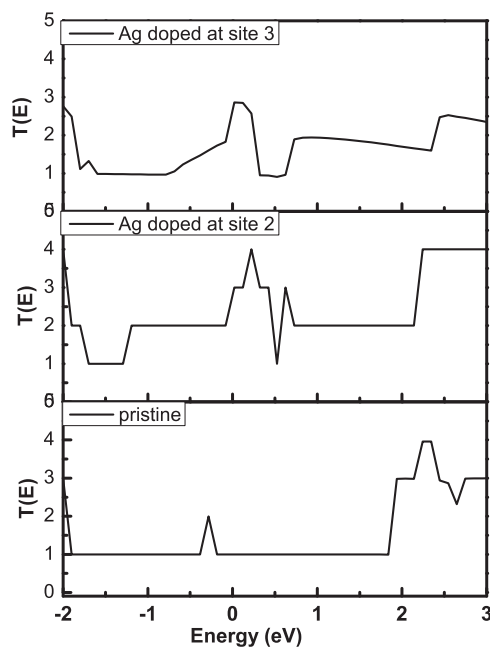


Figure 7. The T.S of the pristine ribbon is compared with Ag doped ZGNRs at zero bias.

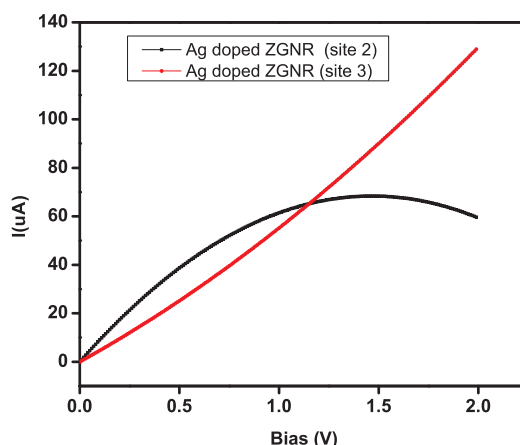


Figure 8. Variation of current as a function of applied voltage for pristine and Ag-doped ZGNR.

4. Conclusion

Doping GNRs with coinage metals reveals interesting I-V characteristics of Cu-doped GNRs with regions of linearity, negative differential regions and saturations. Varying positions of Cu dopant, we predict Cu-doped ZGNRs offer moderate conductances whereas AGNRs offer enhanced conductance along with negative differential conductance. The spin-oriented band gaps of Au-substituted and Au-adsorbed ZGNR indicate that the doping of Au atoms through various methods considerably alters the electronic structure of ZGNRs. Further, adsorption of Au in AGNRs introduces spin-polarized electrons into the non-magnetic semiconductor through an applied bias. Interaction between Ag impurities and edge states of ZGNRs brings sharp electronic activity on doping the ZGNR with Ag at the identified sites. Therefore, through our

first-principles calculations, the interaction of Cu, Au and Ag with the GNRs unveils significant electronic interaction between them in the electronic and transport properties.

Acknowledgement

The authors are thankful to the Council of Scientific and Industrial Research (CSIR), New Delhi for the financial assistance (Project No. 03(1202)/12/EMR-II) and the Computational Nanoscience and Technology Laboratory (CNTL), ABV-Indian Institute of Information Technology and Management, Gwalior for the computational and infrastructural facilities.

Competing Interests

The authors declare that they have no competing interests.

Authors' Contributions

All the authors contributed significantly in writing this article. The authors read and approved the final manuscript.

References

- [1] H. Terrones, R. Lv, M. Terrones and M.S. Dresselhaus, *Rep. Prog. Phys.* **75** (6), 062501 (2012).
- [2] J. Lan, X.H. Zheng, L.L. Song, R.N. Wang and Z. Zhang, *Solid State Commn.* **152**, 1635 (2012).
- [3] G. Yu et al., *J. Phys. D Appl. Phys.* **46** (37), 375303 (2013).
- [4] <http://www.quantumwise.com/>
- [5] B.H. Zhou, W.H. Liao, B.L. Zhou, K.Q. Chen and G.H. Zhou, *Eur. Phys. J. B* **76**, 421 (2010).
- [6] C. Cao, L.N. Chen, D. Zhang, W.R. Huang, S.S. Ma and H. Xu, *Solid State Commn.* **152**, 45 (2012).
- [7] H. Cheraghchi, *Physica Scripta* **84**, 015702 (2011).
- [8] R. Varns and P. Strange, *J. Phys.: Condens. Matter* **20** (22), 225005 (2008).
- [9] J.M. Xu, X.H. Hu, J. Sun, K.B. Yin, S.Y. Lei and L.T. Sun, *Proc. 8th Intl. Vacuum Electron Sources Conference and NANO Carbon* (2010).
- [10] N. Gorjizadeh and Y. Kawazoe, *Materials Trans.* **49** (11), 2445-2447 (2008).
- [11] A. Ishii, M. Yamamoto, H. Asano and K. Fujiwara, *J. Phys. Conf. Series* **100** (5), 052087 (2008).